Low atmospheric CO_2 levels during the Permo-Carboniferous glaciation inferred from fossil lycopsids

D. J. Beerling*

Department of Animal and Plant Sciences, University of Sheffield, Sheffield S10 2TN, United Kingdom

Earth history was punctuated during the Permo-Carboniferous [300–250 million years (Myr) ago] by the longest and most severe glaciation of the entire Phanerozoic Eon. But significant uncertainty surrounds the concentration of CO_2 in the atmosphere through this time interval and therefore its role in the evolution of this major prePleistocene glaciation. Here, I derive 24 Late Paleozoic CO_2 estimates from the fossil cuticle record of arboresecnt lycopsids of the equatorial Carboniferous and Permian swamp communities. Quantitative calibration of Late Carboniferous (330–300 Myr ago) and Permian (270–260 Myr ago) lycopsid stomatal indices yield average atmospheric CO_2 concentrations of 344 ppm and 313 ppm, respectively. The reconstructions show a high degree of self-consistency and a degree of precision an order of magnitude greater than other approaches. Low CO_2 levels during the Permo-Carboniferous glaciation are in agreement with glaciological evidence for the presence of continental ice and coupled models of climate and ice-sheet growth on Pangea. Moreover, the Permian data indicate atmospheric CO_2 levels were low 260 Myr ago, by which time continental deglaciation was already underway. Positive biotic feedbacks on climate, and geotectonic events, therefore are implicated as mechanisms underlying deglaciation.

fossil plants | paleoclimates | stomata | carbon isotopes

Paleobotanical approaches for quantitatively estimating the pre-Quaternary CO_2 content of the Earth's atmosphere exploit the inverse relationship between leaf stomatal index (SI, fraction of epidermal cells that are stomata) and CO_2 shown by modern trees (1). However, their application has focused on the Cretaceous and Early Tertiary when extant species are represented in the fossil record (2). Attempts to extend this approach further back into the Paleozoic era with the genus *Ginkgo* are much less secure because of the need to switch to related taxa, such as pteridosperm genera, whose SIs lie outside the range of the calibration dataset (3). These considerations severely limit the utility of the plant fossil record for evaluating the role of CO_2 as a greenhouse gas during the Late Paleozoic glaciation (4), a time when quite large discrepancies are evident between geochemical modeling studies of the long-term carbon cycle (5), and paleobiological proxy CO_2 measurements (3, 6).

Here, I report 24 quantitative Carboniferous and Permian atmospheric CO_2 estimates derived from the stomatal characteristics of fossil arborscent lycopsids, the spore-bearing vascular plant group dominating equatorial Euramerican and Cathaysian coal swamp floras during the Late Palaeozoic (7). The fossil lycopsid SIs were calibrated against the response to atmospheric CO_2 variations of three geographically distinct contemporary tropical *Lycopodium cernuum* populations, taken to be a reasonable nearest living equivalent (NLE) taxon among extant lycopsid species (8). Phylogenetically, *Isoetes* represents the nearest living relative to members of the *Lepidodendron*, *Bothrodendron*, and *Sigillaria* etc. However, modern *Isoetes* species have either submergent, or emergent growth habits, which are unlikely to sensitively record global changes in atmospheric CO_2 levels. *L. cernuum* fulfils those criteria of an NLE set out

previously (8) because it occupies a comparable ecological setting to its Late Paleozoic arborescent counterparts, with both groups of organisms being characterized by a subtropical/tropical distribution, a preference for open, disturbed habitats, an erect growth habit, and possession of the same microphyll leaf structure. In addition, stable carbon isotope analyses of the organic carbon sources were used to more directly test the similarity of leaf gas exchange metabolism between the extinct and extant lycopsids before estimating paleo-CO_2 levels with the ancient lycopsids.

Materials and Methods

Stable Carbon Isotope Analyses. Stable carbon isotope analyses were performed on herbarium shoots of *L. cernuum* and fossil lycopsids shoots assigned to the Lepidodendraceae, Sigillariaceae, and Bothrodendraceae. Fossil materials were handled with forceps, etched from the rock surface, finely powdered, and reacted with 38% HCl for 24 h, to remove possible carbonate contamination. Samples were then resuspended in deionized water, and centrifuged, and the residual pellet was dried for 72 h at 80°C. Stable carbon isotope ratios were measured by introducing 1 mg of powdered samples with a PDZ Europa ANCA-GSL preparation module into a PDZ Europa (Cheshire, U.K.) 20–20 stable isotope ratio mass spectrometer. Replicate analyses with the same instrument on the same specimens had a reproducibility of 0.5‰. All values are expressed as $[R_{sample} - (R_{sample}/R_{standard}) \times 1,000]$, where R_{sample} is the $^{13}C/^{12}C$ ratio of each sample and $R_{standard}$ is the Pee Dee Belemnite standard.

Fossilized bulk organic carbon is characteristically isotopically less negative by 1–2‰ compared with modern materials, due to the preferential loss of ^{13}C-rich compounds during diagenesis (9). Therefore all fossil plant δ_p measurements were corrected by a conservative 1‰ to account for this effect and facilitate comparison with isotope ratios of herbarium samples.

To isolate isotopic variations due to the biological characteristics of the organisms (10, 11), isotopic discrimination (Δ) was calculated from $(\delta_a - \delta_p)/(1 + \delta_p/1,000)$, where δ_a is the isotopic composition of atmospheric CO_2, estimated from marine calcium carbonate fossils (12). This approach assumes δ_a is regulated on a long-term basis by equilibrium with marine inorganic carbon, with a 7‰ negative offset. Carbon isotope stratigraphies for the interval 320–300 million years (Myr) ago differ somewhat between Panthalassan and Paleotethyan regions, probably due to changes in oceanic circulation associated with the closure of the seaway between Laurussia and Gondwana (12). Here, a mean marine inorganic carbon value from both regions (+5‰) was used, giving $\delta_a = -2.0‰$ for the Westphalian. The ratio of atmospheric CO_2 in the leaf intercellular air spaces (c_i) relative to the air surrounding the leaf (c_a), was then calculated from Δ by rearrangement of the well-validated model
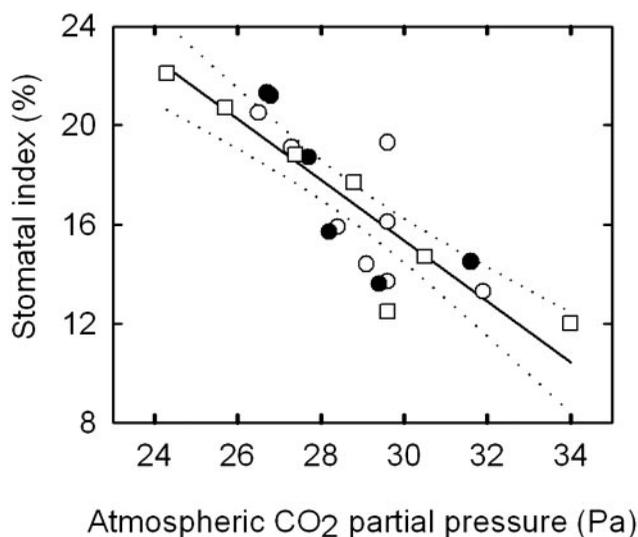

GEOLOGY

Fig. 1. Relationship between SI (fraction of epidermal cells that are stomata) and atmospheric CO_2 partial pressure of different tropical populations of *L. cernuum*. Solid line denotes the linear regression, dotted lines indicate the ±95% confidence limits. Central America (●), South America (□), and Asia (●) (n = 21, $r^2 = 0.73$, $P < 0.01$). All leaves were obtained from the herbarium of the Natural History Museum, London. SI measurements were made on cleared leaves (n = 5–8 per date) of each species collected over the past 150 years of CO_2 increase. Corresponding mean global atmospheric CO_2 concentrations were determined from ice core studies (13) or instrumental records (available at http://cdiac.esd.ornl.gov), after appropriate correction for altitude.

linking Δ to leaf gas exchange (10) by $a + (b - a) \times c_i/c_a$, where *a* and *b* are the fractionations associated with diffusion (4.4‰) and carboxylation by Rubisco (27‰), respectively.

Paleozoic Atmospheric CO₂ Reconstructions. A training set was developed with historical time series of leaves of *L. cernuum* collected since the early 19th century, as atmospheric CO_2 levels increased (13), and from multiple altitudinal transects encompassing spatial gradients of atmospheric CO_2 partial pressure. Leaves of *L. cernuum* were obtained from populations originating in Central America, tropical South America, and the Malaysian Peninsula of southern Asia to assess the response to a global CO_2 signal and account for possible genotypic heterogeneity in the response. The inverse regression transfer function describing the collective SI response (SI,%) of *L. cernuum* populations (Fig. 1) is given by: CO_2 (Pa) = [(SI − 52.259)/ −1.2305]. It is conceivable that leaves of *L. cernuum* respond to CO_2 levels above the global mean, because of the potential for soil-respired CO_2 to accumulate beneath tropical forest canopies. However, CO_2 measurements in tropical forests (14) indicate that at 1–2 m above the soil surface, the height attained by *L. cernuum*, this effect is small (<5%). The occurrence of *L. cernuum* on disturbed, exposed sites suggests these plants grew under irradiance levels similar to those experienced by arborescent lycopods, which with their "pole habit" and unusual canopy architecture (7), may have experienced irradiance levels characteristic of an open habitat.

To quantitatively reconstruct atmospheric CO_2 levels in the Late Paleozoic, SI determinations were made from stomatal and epidermal cell measurements on fossil cuticles of a wide range of tropical lowland arborescent lycopsids from European mid-to-late Carboniferous (15–19) deposits. Estimates of CO_2 in the Permian were based on published SI values of equatorial arborescent lycopsids from deposits in North Chinese upper Permian sections (20) (Table 1). The modern training set captures 70% of the SI values of fossil cuticles (Table 1) despite differences in stomatal placement (leaf cushions of arborescent lycopsids rather than leaves of *L. cernuum*). Observations for *Ulodendron majus* and *Ulodendron landsbergii* suggest the SI of leaves is

Table 1. Stomatal characteristics of fossil Carboniferous (C) and Permian (P) lycopsid microphyll leaves and leaf bases

Fossil specimen	Period	Stage	Age, Myr ago	Organ	SI*, %	Atmospheric CO_2 concentration (ppm) ± 95% cls
Lepidodendron rhodianum	C	Namurian	331–318	Leaf scars	4.9	$385 \pm_{35}^{33}$
L. veltheimii	C	Namurian	331–318	Leaf cushions	4.0	$392 \pm_{35}^{32}$
Lepidophloios grangeri	C	Namurian	331–318	Leaf cushions	8.1	$359 \pm_{34}^{31}$
Bothrodendron minutifolium	C	Westphalian	318–303	Leaves	9.4	$348 \pm_{34}^{31}$
Lepidodendron aculeatum	C	Westphalian	318–303	Leaf cushions	9.0	$351 \pm_{33}^{31}$
L. arberi	C	Westphalian	318–303	Leaf cushions	10.9	$336 \pm_{33}^{30}$
L. dichotomum	C	Westphalian	318–303	Leaf cushions	14.4	$308 \pm_{33}^{30}$
L. feistmantelii	C	Westphalian	318–303	Leaf cushions	9.2	$350 \pm_{34}^{31}$
L. mannabachense	C	Westphalian	318–303	Leaf scars	7.3	$366 \pm_{35}^{32}$
L. peachii	C	Westphalian	318–303	Leaf scars	6.9	$368 \pm_{34}^{31}$
L. subdichotomum	C	Westphalian	318–303	Leaf cushions	8.2	$358 \pm_{34}^{31}$
Lepidophloios acadianus	C	Westphalian	318–303	Leaf cushions	15.0	$303 \pm_{33}^{29}$
L. acerosus	C	Westphalian	318–303	Leaf cushions	7.1	$367 \pm_{35}^{33}$
L. laricinus	C	Westphalian	318–303	Leaf cushions	9.2	$350 \pm_{35}^{33}$
L. macrolepidotus	C	Westphalian	318–303	Leaf cushions	2.9	$401 \pm_{35}^{33}$
Ulodendron landsbergii	C	Westphalian	318–303	Leaf cushions	17.0	$287 \pm_{34}^{32}$
U. landsbergii	C	Westphalian	318–303	Leaves	14.0	$311 \pm_{34}^{32}$
U. majus	C	Westphalian	318–303	Leaf cushions	17.3	$284 \pm_{32}^{30}$
U. majus	C	Westphalian	318–303	Leaves	12.3	$325 \pm_{32}^{31}$
Synchysidendron sp.	P	Kazanian	268	Leaf cushions	10.1	$342 \pm_{34}^{32}$
Paralycopodites sp.	P	Kazanian	266	Leaf cushions	12.1	$326 \pm_{32}^{32}$
Dispersed cuticles	P	Kazanian	263	Leaf cushions (?)	16.6	$290 \pm_{32}^{30}$
Synchysidendron baodeense	P	Kazanian	260	Leaf cushions	10.1	$343 \pm_{34}^{32}$
Dispersed cuticles	P	Kazanian	260	Leaf cushions (?)	19.6	$266 \pm_{30}^{29}$

*Calculated as (SD/(SD + ED) × 100), where SD is stomatal density (mm^{-2}), measured directly on fossil cuticles, and ED is epidermal cell density, calculated from cell dimensions for the Carboniferous plant cuticles.

Table 2. Carbon isotope characteristics of Carboniferous compression fossil lycopsid shoots

Fossil specimen	Specimen number	Organ	δ_{pcorr}, ‰	Δ, ‰	c_i/c_a, unitless
Bothrodendraceae					
Bothrodendron minutifolium	RC2872	Leafy shoot	−23.5	22.0	0.78
B. minutifolium	51813	Leafy shoot	−24.0	22.5	0.80
B. minutifolium	1292	Leafy shoot	−23.4	21.9	0.77
B. minutifolium	1300	Leafy shoot	−22.9	21.4	0.75
B. minutifolium	1201	Leafy shoot	−23.6	22.1	0.78
Lepidodendraceae					
Lepidostrobophyllum alatum	RC4838	Reproductive shoot	−23.1	21.6	0.76
L. lanceolatum	RC3134	Reproductive shoot	−22.9	21.4	0.75
Lepidophyllum sp.	6127	Reproductive shoot	−23.0	21.5	0.76
Lepidodendron ophiurus	5284	Leafy shoot	−23.3	21.8	0.77
L. lanceolatum	JP218	Leafy shoot	−23.9	22.4	0.80
L. lycopodioides	18239	Leafy shoot	−23.2	21.7	0.77
Lepidostrobus sp.	6276	Reproductive shoot	−24.1	22.6	0.81
Sigillariaceae					
Sigillariostrobus rhombibracteatus	1177	Cone	−23.0	21.5	0.76
Sigillariostrobus sp.	1656	Cone	−23.7	22.2	0.79
Sigillaria mamillaris	RC2875	Leafy shoot	−22.7	21.2	0.74
Other lycopsids					
Cyperites bicarinatus	4907	Leafy shoot	−24.7	23.3	0.84
C. bicarinatus	RG4477	Leafy shoot	−24.3	22.9	0.80
C. ciliatum	76313	Leafy shoot	−24.5	23.1	0.83

All specimens are of Westphalian age (303–318 Myr BP) and held at the British Geological Survey, Keyworth, United Kingdom.

20–30% lower than that of leaf cushions (Table 1). If this effect is systematic across all taxa, it translates into an underestimation of atmospheric CO_2 levels of 7–10%. Paleo-CO_2 values have been expressed in this article as concentration, since at sea level, where the Carboniferous and Permian tropical swamp forests were located, CO_2 concentration is equivalent to partial pressure (1 Pa $\approx$ 10 ppm).

Results and Discussion

Physiological Comparisons. Comparative stable carbon isotope analyses allow a first-order test of the assumed physiological similarities between extinct and extant lycopsid taxa by providing an indicator of the set point of photosynthetic metabolism (11) between the two groups of organisms. It emerges that the range of carbon isotope discrimination (Δ) values of fossils (Table 2) is within the variation displayed by the three geographically separated tropical populations of *L. cernuum* (Fig. 2). With Δ values of $\approx$20–22‰, the arborescent lycopsids display operational set points of leaf gas exchange activity similar to those of *L. cernuum*, which indicates a rather low (<27%) diffusional limitation on photosynthesis, a likely consequence of their relatively high SIs (Table 2). The isotopic data suggest that photosynthetic activity and stomatal control of water loss in contemporary *L. cernuum* populations is comparable to that of the ancient Carboniferous lycopsids, despite obvious differences in scale between the two groups of organisms. It should be noted, however, that in one respect the comparison is imperfect because *L. cernuum* in this study experienced a drop in CO_2 partial pressure as a function of altitude (i.e., falling total pressure) whereas the fossils grew at a time when total atmospheric pressure was similar or slight higher than now. If the comparison is taken to be reasonably robust, a further implication is that the physiology of lycopsids has apparently been highly conserved, despite the potential for over 300 Myr of evolutionary change, in a group that also shows a considerable degree of phylogenetic conservatism (21).

Paleozoic CO_2 Reconstructions. Quantitative paleo-CO_2 reconstructions obtained by calibration of the fossil SI values show consistent and tightly constrained values for the Carboniferous and Permian (Table 1). The assumed CO_2 signal in the fossil lycopsid cuticles is stable within the Namurian (330 and 320 Myr ago) and the Westphalian (320–300 Myr ago) stages of the Carboniferous and gives mean global values of 379 ppm and 336 ppm, respectively. These results are supported by two qualitative estimates of CO_2 obtained by analysis of fossil conifers dating to the Carboniferous and early Permian (22). Within the Westphalian, the record exhibits a strong degree of self-consistency, with leaves of four extinct families of arborescent lycopods all giving similar CO_2 estimates (Table 1). Low atmospheric CO_2 levels prevailing during the Late Carboniferous are reconstructed for the Permian, with lycopsids from North China yielding a mean value of 313 ppm between $\approx$270 and 260 Myr ago (Table 1).

The paleoatmospheric CO_2 values for the Carboniferous span 30 Myr and are consistent with low levels of net radiative forcing
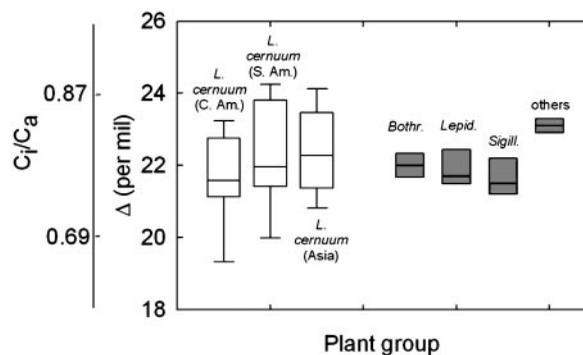

Fig. 2. Comparison of the carbon isotope discrimination ($\triangle$) of modern ($\square$) and extinct ($\blacksquare$) lycopsids. Each box delineates the 25th and 75th percentiles, errors bars show the fifth and 95th percentiles, the horizontal line represents the median value of the sample set. Δ calculated for herbarium leaf sequences of *L. cernuum* (Central America populations, $n = 9$, 1868–1995; South American populations, $n = 8$, 1853–1987; Asian populations, $n = 12$, 1822–1981). Changes in Δ were not correlated with historical atmospheric CO_2 increase in the extant lycopsid species. Therefore, intraspecific variations reflect differences in microhabitats and interannual climate fluctuations.
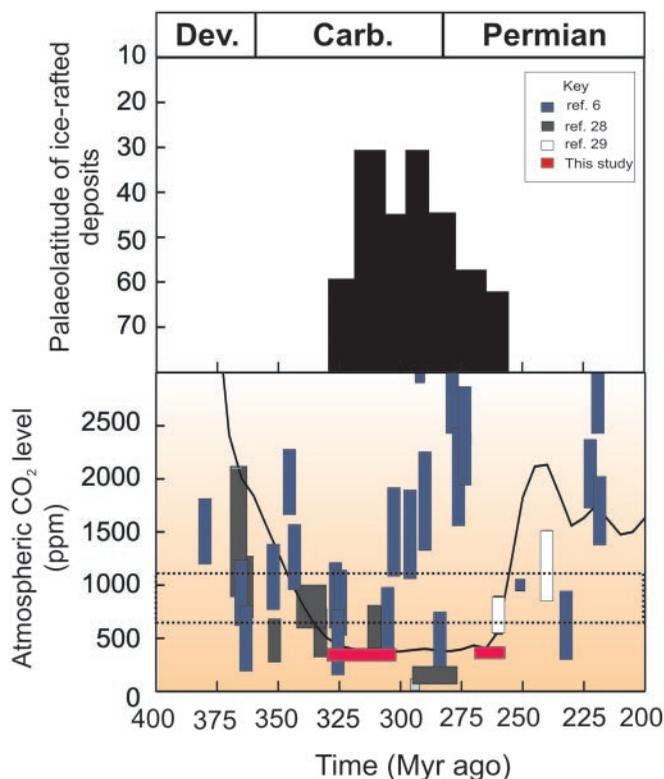
GEOLOGY

Fig. 3. Late Palaeozoic evidence for ice (summarized from refs. 23, 25, and 27) and atmospheric CO_2 concentrations reconstructed from paleosols and predicted by a geochemical model of the long-term global carbon cycle (solid line). Red boxes indicate CO_2 estimates from the current study. The dashed horizontal line indicates the threshold atmospheric CO_2 level above which theoretical studies predict deglaciation on Pangea and the maintenance of an ice-free state (24).

(23, 24) and the occurrence of major ice sheets on Gondwana (25, 26). Further, the CO_2 reconstructions are tightly constrained and have an order of magnitude greater precision (95% confidence limits $\pm \approx 35$ ppm) than carbon cycle models and paleosols, which are subject to larger (± 200 ppm and $\pm 500–1,000$ ppm, respectively) error terms for this interval (27). They therefore narrow a significant uncertainty in the role played by atmospheric CO_2 during the Permo-Carboniferous glaciation (4, 23, 25, 26). My CO_2 estimates are in agreement with the lower set of values predicted by geochemical carbon cycle modeling studies (5) and reconstructed from isotopic analyses of Late Paleozoic North American paleosols (28) (Fig. 3).

Implications for the Mechanisms of Deglaciation. The Permian CO_2 data shed some light on the role of atmospheric CO_2, as a

greenhouse gas, in the closing phase of the Late Paleozoic glaciation, a subject of considerable debate (3–6). Paleosol studies suggest low CO_2 concentrations (150–200 ppm) 280 Myr ago (28), and all five Permian lycopsid SIs indicate that atmospheric CO_2 levels were also low between 268 and 260 Myr ago with values reconstructed to be ≈ 313 ppm (Table 1). These results are generally supported by geochemical modeling (5), but are lower than CO_2 estimates from Permian paleosols in Central India dating to 260 Myr ago (540–890 ppm) (29). They fail to support the contention (3, 6) that atmospheric CO_2 levels were high around 260 Myr ago. However, the interpretation of high Late Permian CO_2 levels (1,000–2,000 ppm) reconstructed from paleosols (6) depends on the isotopic composition of marine carbonates (30). Calculated with the paleosol CO_2 barometer by using an alternative marine isotopic record (12) to that of ref. 31 results in a considerable damping of this CO_2 rise, with values lower by some 700–2,500 ppm (27). High Permian atmospheric CO_2 levels inferred from the SI of peltasperm seed ferns (3) appear to be compromised by dating imprecision, taxonomic uncertainties, and inadequate replication (32).

If atmospheric CO_2 concentrations were low toward the close of the Permian, when a variety of geological data suggest deglaciation was well underway (23, 25, 26), then climatic forcing factors other than high levels of CO_2 in the atmosphere may need to be examined to determine the cause of the Late Paleozoic deglaciation. Evidence for plate tectonic activity indicates that the southern Gondwana drifted across the South Pole during the Carboniferous and Permian, 320–260 Myr ago (33). This clockwise rotation of the plates would have exposed the Gondwana supercontinent ice masses to latitude-controlled warmer climates, leading directly to melting of the ice sheets (26), without the need to invoke changes in the concentration of greenhouse gases. Moreover, as *Glossopteris* floras spread into areas previously covered by ice (34), a positive feedback would have ensued due to seasonal reductions in land surface albedo, as the ice became replaced with a forested landscape. The switch in land cover from ice to forest has been found in contemporary climate modeling studies to be an effective promoter of strong high latitude climatic warming (35). In fact, numerical modeling simulations of early Permian climates lack representation of this vegetation feedback and it is notable that they have yet to satisfactorily reproduce the distribution of fossilized biota in the high southern latitudes, even when high ($8 \times$ times modern) atmospheric CO_2 concentrations are prescribed (36).

1. Woodward, F. I. (1987) *Nature (London)* **327,** 617–618.
2. Royer, D. L., Wing, S. L., Beerling, D. J, Jolley, D. W., Koch, P. L., Hickey, L. J. & Berner, R. A. (2001) *Science* **292,** 2310–2313.
3. Retallack, G. J. (2001) *Nature (London)* **411,** 287–290.
4. Crowley, T. J. & Baum, S. K. (1992) *Geology* **20,** 507–510.
5. Berner, R. A. & Kothavala, Z. (2001) *Am. J. Sci.* **301,** 182–204.
6. Ekart, D., Cerling, T. R., Montanez, I. P. & Tabor, N. J. (1999) *Am. J. Sci.* **299,** 805–827.
7. Phillips, T. L. & DiMichele, W. A. (1992) *Ann. Missouri Bot. Gard.* **79,** 560–588.
8. McElwain, J. C. & Chaloner, W. G. (1995) *Ann. Bot.* **76,** 389–395.
9. Benner, R., Fogel, M. L., Kent Sprague, E. & Hodson, R. E. (1987) *Nature (London)* **329,** 708–709.
10. Farquhar, G. D., Eherlinger, J. R. & Hubrick, K. T. (1989) *Annu. Rev. Plant Physiol. Mol. Biol.* **40,** 503–537.
11. Ehleringer, J. J. (1994) in *Ecophysiology of Photosynthesis*, eds. Schulze, E. D. & Caldwell, M. M. (Springer, Berlin), pp. 363–392.

12. Mii, H. S, Grossman, E. L. & Yancey, T. E. (1999) *Geol. Soc. Am. Bull.* **111,** 960–973.
13. Friedli, H., Lötscher, H., Oeschger, H., Siegenthaler, U. & Stauffer, B. (1986) *Nature (London)* **324,** 237–238.
14. Broadmeadow, M. S. J. & Griffiths, H. (1993) in *Stable Isotopes and Plant Carbon-Water Relations*, eds. Ehleringer, J. R., Hall, A. E. & Farquhar, G. D. (Academic, San Diego), pp. 109–129.
15. Thomas, B. A. (1967) *Ann. Bot.* **31,** 775–782.
16. Thomas, B. A. (1968) *J. Nat. Hist.* **2,** 425–428.
17. Thomas, B. A. (1967) *J. Nat. Hist.* **1,** 53–60.
18. Thomas, B. A. (1977) *Palaeontology* **20,** 273–293.
19. Thomas, B. A. (1970) *Palaeontology* **13,** 145–173.
20. Wang, Z. & Chen, A. (2001) *Rev. Palaeobot. Palynol.* **117,** 217–243.
21. Wikstrom, N. & Kenrick, P. (2001) *Mol. Phylogen. Evol.* **19,** 177–186.
22. McElwain, J. C. & Chaloner, W. G. (1996) *Palaios* **11,** 376–388.
23. Crowley, T. J. & Berner, R. A. (2001) *Science* **292,** 870–872.

24. Hyde, W. T., Crowley, T. J., Tarasov, L. & Peltier, W. R. (1999) *Climate Dynamics* **15,** 619–629.
25. Frakes, L. A. & Francis, J. E. (1988) *Nature (London)* **333,** 547–549.
26. Crowell, J. C. (1999) *Pre-Mesozoic Ice Ages: Their Bearing On Understanding The Climate System* (Geological Society of America, Boulder, CO), Memoir 192.
27. Royer, D. L., Berner, R. A. & Beerling, D. J. (2001) *Earth Sci. Rev.* **54,** 349–392.
28. Mora, C. I., Driese, S. G. & Colarusso, L. A. (1996) *Science* **271,** 1105–1107.
29. Ghosh, P., Ghosh, P. & Bhattacharya, S. K. (2001) *Palaeogeogr. Palaeoclimatol. Palaeoecol.* **170,** 219–236.
30. Cerling, T. E. (1992) *Global Biogeochem. Cycles* **6,** 307–314.
31. Veizer, J., Ala, D., Azmy, K., Bruckschen, P., Buhl, D., Bruhn, F., Carden, G. A. F., Diener, A., Ebneth, S., Godderis, Y., *et al.* (1999) *Chem. Geol.* **161,** 59–88.
32. Kerp, H. (2002) *Nature (London)* **415,** 38.
33. Powell, C. McA. & Li, Z. (1994) in *Permian-Triassic Pangean Basins and Foldbelts Along the Panthalassan Margin of Gondwanaland*, eds. Veevers, J. J. & Powell, C. M. (Geological Society of America, Boulder, CO), Memoir 184, pp. 5–9.
34. Chaloner, W. G. & Lacey, W. S. (1973) *Special Papers Palaeontol.* **12,** 271–289.
35. Bonan, G. B., Pollard, D. & Thompson, S. L. (1992) *Nature (London)* **359,** 716–718.
36. Rees, P. M., Ziegler, A. M., Gibbs, M. T., Kutzbach, J. E., Behling, P. J. & Rowley, D. B. (2002) *J. Geol.* **110,** 1–31.

GEOLOGY